Two K^+ Channel Types, Muscarinic Agonist-activated and Inwardly Rectifying, in a Cl^- Secretory Epithelium: the Avian Salt Gland

NEIL W. RICHARDS, R. JOEL LOWY, STEPHEN A. ERNST, and DAVID C. DAWSON

From the Departments of Physiology and of Anatomy and Cell Biology, University of Michigan Medical School, Ann Arbor, Michigan 48109

ABSTRACT Patches of membrane on cells isolated from the nasal salt gland of the domestic duck typically contained two types of K^+ channel. One was a large-conductance ("maxi") K^+ channel which was activated by intracellular calcium and/or depolarizing membrane voltages, and the other was a smaller-conductance K^+ channel which exhibited at least two conductance levels and displayed pronounced inward rectification. Barium blocked both channels, but tetraethylammonium chloride and quinidine selectively blocked the larger K^+ channel. The large K^+ channel did not appear to open under resting conditions but could be activated by application of the muscarinic agonist, carbachol. The smaller channels were open under resting conditions but the gating was not affected by carbachol. Both of these channels reside in the basolateral membranes of the Cl^- secretory cells but they appear to play different roles in the life of the cell.

INTRODUCTION

The avian salt gland is an extrarenal salt excretory tissue which has been used to investigate the molecular events involved in the regulation of epithelial salt secretion. Glandular secretion is under the control of cholinergic nerve fibers (Peaker and Linzell, 1975) and muscarinic receptors have been characterized in the isolated cells (Hootman and Ernst, 1982). Activation of these receptors by muscarinic agonists stimulates ouabain-sensitive respiration and phosphoinositide turnover, and increases intracellular calcium concentration (Hokin and Hokin, 1967; Hootman and Ernst, 1980, 1981; Snider et al., 1986). When confluent sheets of salt gland cells are grown in primary culture and mounted in Ussing chambers, carbachol stimulates a net serosal-to-mucosal Cl^- flux and promotes a furosemide- and

Address reprint requests to Dr. Neil W. Richards, Department of Physiology, University of Michigan Medical School, 6812 Medical Science II, Box 0622, Ann Arbor, MI 48109.
Dr. Lowy's current address is Physiology Department, Armed Forces Radiobiology Research Institute, Bethesda, MD 20814.

J. GEN. PHYSIOL. © The Rockefeller University Press · 0022-1295/89/06/1171/24 $2.00
Volume 93 June 1989 1171–1194

ouabain-sensitive short-circuit current (I_{sc}) in a manner consistent with active Cl^- secretion (Lowy et al., 1985*a*, 1989).

The present study was prompted by the observation that barium, a K^+-channel blocker, abolished the secretagogue-induced I_{sc} in salt gland cultures when added to the basolateral side of the cell layer (Lowy et al., 1989). This finding suggests the involvement of basolateral K^+ channels in the secretory process. Our aim was to apply single-channel recording techniques to isolated salt gland cells in order to identify and characterize the single K^+ channels which might participate in the secretory response. We found that salt gland cell membranes contained two distinct populations of K^+-selective channels and that both channel types were typically present in most membrane patches. The channels could be distinguished by several criteria including their differential sensitivity to tetraethylammonium chloride (TEA) and other K^+-channel blockers. Our findings indicate that these two channel types could play different roles in the activity of salt gland cells. One, a large-conductance, Ca^{2+}-activated K^+ channel, was activated by muscarinic agonists but did not appear to play a major role in determining the resting membrane potential. The other, a smaller-conductance, inwardly rectifying K^+ channel, was unaffected by carbachol but could play a role under resting or unstimulated conditions.

METHODS

Cell Isolation

Avian salt gland cells were isolated according to methods previously described in detail (Lowy et al., 1985*b*). Briefly Pekin ducklings (*Anas platyrhyncos*) were osmotically stressed by addition of 1% NaCl to their drinking water for a period ranging from 2 d to 5 wk. Salt stress causes the salt gland to hypertrophy and the epithelial cells to differentiate, a process which results in extensive infolding of the basolateral membranes (Ernst and Ellis, 1969). Salt glands were then removed and dissociated by enzymatic disruption of the extracellular matrix. This method yields large, highly pure quantities of single epithelial cells which retain ultrastructural integrity, normal intracellular ion content, and responsiveness to cholinergic agonists (Hootman and Ernst, 1980, 1981, 1982; Lowy et al., 1985*b*; Snider et al., 1986). Salt gland cells in the isolated state assume a more or less spherical shape, although basolateral infolding remains apparent (Hootman and Ernst, 1980; Lowy et al., 1985*b*). The apical surface, whose area is small compared to the extensive basolateral membrane (Ernst and Ellis, 1969) is not morphologically distinguishable in these isolated cells (Hootman and Ernst, 1980; Lowy et al., 1985*b*).

Primary Culture

Avian salt gland cells were grown in primary culture as described previously (Lowy et al., 1985*b*). For the purpose of patch clamping, cells were seeded onto glass coverslips which had been coated with collagen (Vitrogen 100, Collagen Corp., Palo Alto, CA).

Patch-Clamp Procedure

Pipette electrodes were fabricated from Kimble No. R6 glass (Kimble Glass, Vineland, NJ, obtained through Richland Glass, Richland, NJ) and tips were coated with polystyrene Q-Dope (GC Electronics, Rockford, IL) to reduce capacitance. Salt gland cells were placed in a 1–2-ml glass-bottomed chamber on the stage of an inverted microscope (Diaphot; Nikon,

Inc., Garden City, NY) and viewed at ×600 under Nomarski optics. The microscope was positioned on a vibration-isolated lab bench (Newport Corp., Fountain Valley, CA) and enclosed in a stainless steel Faraday cage to prevent mechanical and electrical interference. High-resistance seals were formed to cell membranes according to the technique of Hamill et al. (1981) and membrane patches were voltage clamped using an Axopatch 1A or 1B patch-clamp amplifier (Axon Instruments, Inc., Burlingame, CA). Holding potential (V_h) was defined as the potential at the cell interior, with respect to that of the pipette. Current output was digitized using a modified digital audio processor (Benzanilla, 1985) and the digitized record stored on videocasette tape for later analysis.

Solutions

Solutions used were based on Earle's balanced salt solutions (EBSS) and included NaCl-EBSS (in millimolar: 116 NaCl, 5.4 KCl, 1.0 NaH_2PO_4, 15 *N*-2-hydroxyethylpiperazine-*N'*-2-ethanesulfonic acid [HEPES], 10 *N,N*-bis(2-hydroxyethyl)-2-aminoethanosulfonic acid [BES], 10 *N*-tris(hydroxymethyl)methyl-2-aminomethanesulfonic acid [TES], 10 glucose, 1.0 $MgCl_2$ 1.4 $CaCl_2$; pH 7.4) and KCl-EBSS in which NaCl was replaced with KCl. Ca^{2+}-buffered solutions were used in some experiments and contained (in millimolar): 112 KCl, 2–5 ethylene glycol bis (β-aminoethyl ether)*N,N,N',N'*-tetraacetic acid (EGTA), 10–20 piperazine-*N,N'*-bis (2-ethane-sulfonic acid (PIPES); pH 7.0. Sufficient $CaCl_2$ was added to yield calculated free ionized Ca^{2+} concentrations in the range of 10^{-7} to 10^{-3} M, as described by Chang et al. (1988). All solutions were used at room temperature.

Pharmacological agents were added to the cells by perfusing the appropriate solution containing the agent through the chamber until the bath was completely replaced. Quinidine HCl, carbamylcholine chloride (carbachol) and TEA were purchased from Sigma Chemical Co. (St. Louis, MO).

Data Analysis

Single-channel records were analyzed using an AT (IBM Corp., Danbury, CT) or Multitech 900 (Multi-Tech Systems, Inc., New Brighton, MN) computer with pCLAMP software (Axon Instruments, Inc.) in conjunction with auxiliary programs designed to read pCLAMP files. These auxiliary programs were used to calculate fractional open time and mean current.

Fractional open time. Fractional open time was defined as the fraction of total time that a channel spends in an open state. Single-channel records were analyzed using pCLAMP to construct an idealized record of channel open and closed times. An auxiliary program was then used to calculate fractional open time as the cumulative sum of the open times divided by the sum of the cumulative open plus cumulative closed times. Unless otherwise indicated, current records were low-pass filtered at 1 kHz and digitized at 5 kHz for idealized record construction. This analysis was generally limited to records from patches containing only one active channel. To minimize spurious values of fractional open time resulting from occasional very long closed intervals, the single longest closed interval in each file was usually omitted from the open time calculation.

Mean current. Mean current was defined as the total charge carried through the channels divided by the total time of the channel record. This analysis was applied to current records containing more than one active channel and in other records from which an idealized record could not be accurately determined. The pCLAMP program was modified to define specific sections of digitized current records which represent closed channel baseline. Mean current was calculated as the integral of all digitized current values in the file using the defined baseline as zero current. Appropriate scaling factors were used to express mean current in picoamperes.

RESULTS

We were generally able to obtain high-resistance seals to the membranes of isolated duck salt gland cells despite the extensive basolateral membrane infolding characteristic of this cell type in the differentiated state (Hootman and Ernst, 1980; Lowy et al., 1985*b*). Seals were most consistently formed using pipettes fabricated from Kimble No. R6 glass. Other glasses (Nos. 8161 and 7052; Corning Glass Works, Corning, NY, Kimax-51; Kimble Glass, Boralex; Rochester Scientific Co., Inc., Rochester, NY) were decidedly inferior for this purpose. Two types of single K^+ channels were commonly recorded: one exhibiting a large conductance and other characteristics that identified it as a Ca^{2+}-activated, "maxi" K^+ channel, and another characterized by a smaller conductance and a pronounced inward rectification.

Large-Conductance K^+ Channel

Cell-attached patches. To record single K^+ channels in cell-attached patches, seals were made with NaCl-EBSS (5 mM K^+) in the pipette and KCl-EBSS (121 mM K^+) in the bath. Under these conditions, an outwardly directed K^+ gradient existed across the patch, and the high K^+ concentration in the solution bathing the cells depolarized the resting membrane potential so that the total potential across the patch was approximated by the applied, or holding, potential. Membrane patches on differentiated cells under these conditions typically displayed large outward unitary currents (3.7 ± 1.2 pA, $n = 10$) at a holding potential of 0 mV (Fig. 1). The voltage dependence of this channel (see below) complicated an accurate determination of reversal potential in the cell-attached configuration. However, the apparent null potential for these currents was more negative than −30 to −40 mV, as expected for a K^+-selective channel. The slope conductance determined from nine current-voltage plots under these conditions was 98 ± 6 pS (mean ± SE).

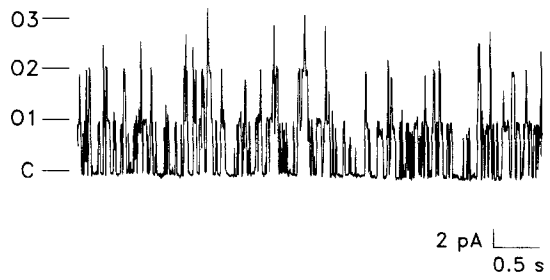

FIGURE 1. Outward K^+ currents of large unitary conductance recorded from duck salt gland cell membranes. Traces were recorded from a cell-attached patch with NaCl-EBSS (5 mM K^+) in the pipette and KCl-EBSS (121 mM K^+) in the bath to depolarize the resting membrane potential. Holding potential was 0 mV. Channel opening is indicated by an upward pen deflection. Markers at left indicate the current level when all channels were closed (*C*) and current levels which represent the opening of up to three channels (*01–03*). Patches containing multiple channels, such as the one shown, were commonly observed.

The gating of the large-conductance K^+ channel in cell-attached patches was strongly dependent on the membrane potential, such that open time increased with membrane depolarization. In K^+-depolarized cells with NaCl-EBSS in the pipette, fractional open time for outward K^+ currents at $V_h = 0$ mV was 0.27 ± 0.08 (mean ± SE) in five patches for which this analysis was performed. Depolarizing the

potential to +20 mV (cell interior positive) increased fractional open time to 0.77 ± 0.13, whereas at −20 mV fractional open time decreased to 0.07 ± 0.03. The change in gating induced by a step change in holding potential occurred with no discernible delay.

Current records under these conditions (i.e., K^+-depolarized cells with NaCl-EBSS in the pipette) were dominated by the large-conductance K^+ channel. The majority of patches contained at least one large K^+ channel and patches containing multiple channels (2–10 or more) were not uncommon. The number of large K^+ channels per patch seemed to be somewhat higher in more highly differentiated cells, e.g., in cells from animals subjected to 3 wk of salt stress compared with animals subjected to only 2 d of salt stress.

Inside-out patches. The large-conductance K^+ channel remained active after excision of the patch from the cell. However, no voltage dependence of channel gating was observed in inside-out patches when the cytoplasmic face of the membrane was bathed with standard EBSS solutions containing 1.4 mM $CaCl_2$. The

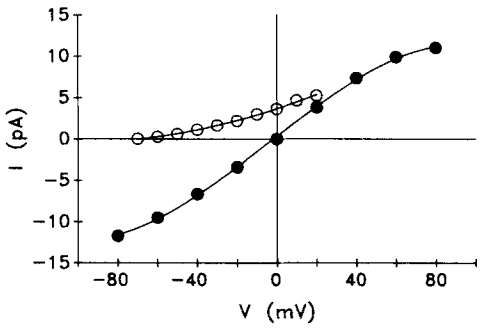

FIGURE 2. Representative current–voltage relations for the large-conductance K^+ channel. Both plots were determined using excised, inside-out patches. Holding potential was defined as the potential at the cell interior. In the presence of an outwardly directed K^+ gradient (○), with KCl-EBSS in the bath and NaCl-EBSS in the pipette, the slope conductance determined from the ohmic portion of the curve in the vicinity of 0 mV was 78 pS and the apparent reversal potential was ~−70 mV. The mean conductance determined from eight such plots was 80 ± 4 pS (±SE). In a separate patch bathed in symmetric KCl-EBSS solutions (●), currents reversed near 0 mV and the slope conductance was 155 pS. The mean conductance determined from nine such plots was 168 ± 2 pS (±SE).

channels in this case remained open a majority of the time at all potentials tested. Currents exhibited a characteristic gating in which the open periods were punctuated by frequent, brief (often unresolved) closings to baseline. The slope conductance of outward currents determined from inside-out patches in the presence of an outwardly directed K^+ gradient (121 mM/5 mM) was ~80 pS and the reversal potential was near −70 mV (Fig. 2). In inside-out patches bathed in symmetric KCl-EBSS solutions, both inward and outward currents were recorded and the *I–V* relation was ohmic over the range of ±60 mV. Slope conductance determined from nine patches under these conditions was 168 ± 2 pS and the reversal potential was near 0 mV. Commonly, brief (<1 s) transitions of the open channel current to distinct subconductance levels ranging between one-third and two-thirds the magnitude of the dominant conductance were observed. We assume that these partial current steps represented subconductance states of the channel and not additional channel types because independent openings of a channel having one of the lower

conductances were never observed. Occasionally, the open channel current remained stable at one of the subconductance levels for several seconds (Fig. 3).

Calcium and voltage dependence in inside-out patches. The first indication that the gating of the large-conductance K^+ channel was Ca^{2+} dependent was a dramatic increase in open time observed when cell-attached patches were excised into standard EBSS solutions containing 1.4 mM $CaCl_2$. The dependence of open time on cytoplasmic Ca^{2+} was quantified by using inside-out patches and bathing the cytoplasmic face of the membrane with solutions containing a Ca-EGTA buffer. Fig. 4 *A* shows the effect of raising the free Ca^{2+} concentration at the inside membrane in a patch containing four large-conductance K^+ channels. The current traces show inward currents recorded from an inside-out patch bathed with symmetric high K^+ solutions at a holding potential of −60 mV. At 1 μM Ca^{2+}, openings were brief and relatively infrequent and the channels spent most of the time in a closed state. Increasing the Ca^{2+} concentration at the cytoplasmic membrane progressively increased the fraction of total time that the channels were open such that at 10 μM Ca^{2+} the channels were largely open. We noted a rather surprising variability of the

FIGURE 3. Trace illustrates an unusually long-lived transition to a subconductance state of the large-conductance K^+ channel, recorded from an inside-out patch bathed with symmetric KCl-EBSS solutions at a holding potential of −60 mV. Channel opening (inward current) is indicated by a downward pen deflection. The current levels to the left of the trace are labeled *C* for closed current level, *O* for the normal fully open current level, and *S* for the subconductance level. In this trace, the channel remained stable at the subconductance level for several seconds. Shorter (<1 s) sojourns in this and other subconductance states were more commonly observed.

ability of Ca^{2+} to activate large-conductance K channels in different patches. Fig. 4 *B* shows the Ca^{2+}-activation profiles for 10 separate patches under the conditions of Fig. 4 *A*. The majority of patches were activated by free Ca^{2+} concentrations ranging from 1 to 10 μM. One patch, however, was more sensitive, being activated maximally by 1 μM Ca^{2+}, while another required up to 1 mM Ca^{2+} for maximal activation.

The gating of the large-conductance K^+ channel in inside-out patches exhibited voltage dependence when the Ca^{2+} concentration at the cytoplasmic membrane was <1 mM. For a given cytoplasmic Ca^{2+} concentration, fractional open time increased as the potential was made more positive at the cell interior. At positive cell potentials, fractional open time remained high even in the presence of a Ca^{2+}-free solution. In inside-out patches bathed with symmetric high K^+ solutions but with an essentially Ca^{2+}-free solution (no added Ca^{2+} + 2–5 mM EGTA) at the inside membrane, fractional open time at −30, +30, and +60 mV was 0.003 ± 0.002, 0.554 ± 0.143, and 0.832 ± 0.249, (mean ± SD, n = 3), respectively.

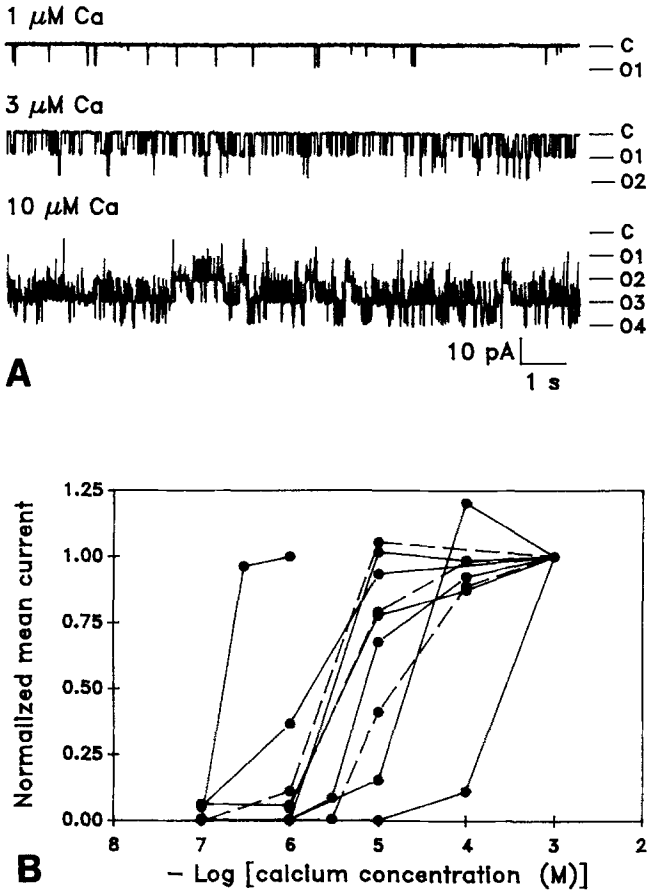

FIGURE 4. (*A*) Effect of Ca^{2+} concentration at the cytoplasmic face of the membrane on currents through the large-conductance K^+ channels. Traces show inward K^+ currents (downward pen deflection) recorded from an inside-out patch which contained four large-conductance K^+ channels. The pipette contained KCl-EBSS and the bath contained a 112 mM KCl solution in which the free Ca^{2+} concentration was buffered with 2 mM EGTA. Holding potential was −60 mV. Markers at left indicate the closed channel current level (*C*) and up to four open channel current levels (*O1–O4*). The amount of time spent in the open state increased progressively as the free Ca^{2+} concentration at the inside membrane was increased in the range of 1–10 μM. (*B*) Calcium activation profiles of the large-conductance K^+ channels in different patches. The figure shows mean current as a function of Ca^{2+} concentration at −60 mV for 10 separate patches from different cells. Mean current for each curve was calculated as the average of four consecutive 10-s segments of records such as those shown in *A* and normalized as a fraction of mean current in the presence of 1.0 mM Ca^{2+} (i.e., mean current in the presence of 1 mM Ca^{2+} = 1.00). The Ca^{2+} sensitivity of the large-conductance K^+ channels showed a surprising variability from cell to cell.

Blocker specificity. Currents through the large-conductance Ca^{2+}-activated K^+ channel were blocked in excised patches by barium, TEA, and quinidine. Barium was the most potent blocker when added to the cytoplasmic face of the membrane. Addition of Ba^{2+} to the solution bathing the inside membrane of inside-out patches caused the appearance of very long, nonconducting (blocked) intervals interspersed with relatively brief bursts of openings (Fig. 5 *A*). Within these opening bursts the normal gating pattern of brief flickery closings was maintained. The efficacy of Ba^{2+} blockade was a function of membrane potential and was greatest at potentials which favored Ba^{2+} entry into the channel. Fig. 5 *B* shows the result of three experiments where Ba^{2+} was added to the inside membrane of inside-out patches bathed in symmetric KCl-EBSS solutions at two potentials. At a positive holding potential (+60 mV), blockade of single-channel currents was significant at a Ba^{2+} concentration as

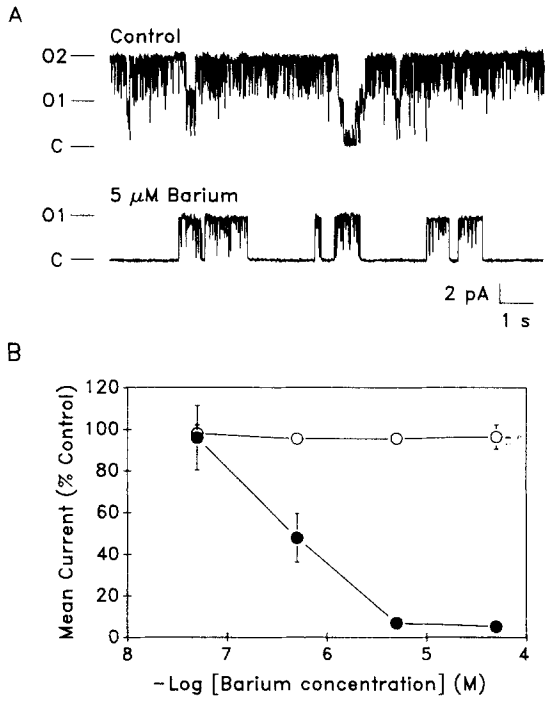

FIGURE 5. Blockade of the large-conductance K^+ channel by intracellular barium. (*A*) Representative outward currents (upward pen deflection) recorded from an inside-out patch with NaCl-EBSS in the pipette and KCl-EBSS in the bath, before and after addition of 5 μM $BaCl_2$ to the bathing solution. Holding potential was 0 mV. Markers at left indicate the closed channel current level (*C*) and current levels which correspond to the opening of two channels (*01–02*). In the absence of Ba^{2+}, the channels in the patch were mainly in an open state due to the presence of a high Ca^{2+} concentration (1.4 mM) at the inside membrane. Addition of 5 μM Ba^{2+} caused the appearance of long nonconducting intervals in the current record, effectively dividing the record into a series of short, opening bursts. Mean current in the presence of 5 μM Ba^{2+} was 15% of control for this particular record. The block by Ba^{2+} was reversed by washing Ba^{2+} out of the bath. (*B*) Voltage dependence of Ba^{2+} block. Mean current was calculated for K^+ currents obtained from an inside-out patch bathed in symmetric KCl-EBSS solutions at a holding potential of −60 mV (○) or +60 mV (●) in the presence of 0.5–50 μM $BaCl_2$ added to the bath. Block of outward current was virtually complete with 5–50 μM Ba^{2+} at +60 mV, whereas little or no block of inward current was observed at −60 mV. Points shown are mean ± SE of three experiments. For each experiment, mean current was determined as the average obtained from four consecutive 10-s segments of current record.

low as 0.5 μM and block was virtually complete at 5–50 μM. Conversely, these same concentrations of Ba^{2+} produced little or no block at a holding potential of −60 mV.

Barium added to the external face of the channel also produced a voltage-dependent block but higher concentrations were required. Fig. 6 *A* shows inward currents recorded from two separate inside-out patches bathed with symmetric KCl-EBSS solutions at a holding potential of −60 mV, one with 5 mM $BaCl_2$ in the pipette solution and the other without Ba^{2+}. In the absence of Ba^{2+}, the channel remained

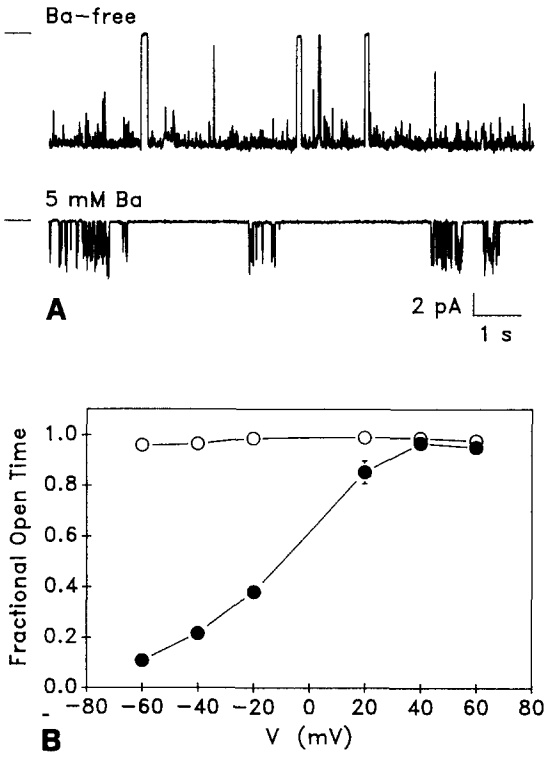

FIGURE 6. Blockade of the large-conductance K^+ channel by external Ba^{2+}. (*A*) The upper trace shows representative inward K^+ currents recorded using inside-out patches bathed in symmetric KCl-EBSS solutions. Holding potential was −60 mV. Markers at left indicate the closed current level. The lower trace is from a similar patch but with 5 mM $BaCl_2$ in the pipette. Currents in the presence of Ba^{2+} contained numerous nonconducting intervals which were not present in patches without Ba^{2+}. In addition, opening bursts displayed flickery behavior and apparent current amplitude was reduced. (*B*) Fractional open time as a function of potential in the presence and absence of Ba^{2+}. In the absence of Ba^{2+} (○), fractional open time was >0.95 at all potentials tested. With 5 mM $BaCl_2$ in the pipette (●), fractional open time was similar to Ba^{2+}-free patches at positive potentials, but decreased as the potential was made more negative at the cell interior. Each point is the mean ± SE of three experiments. Fractional open time for each experiment was determined as the mean of four consecutive 10-s intervals of current record.

open most of the time. Gating was not voltage-dependent due to the presence of a high Ca^{2+} concentration (1.4 mM) at the inside face of the membrane. Traces recorded with 5 mM Ba^{2+} in the pipette solution appeared to display characteristics of both fast and slow block. Opening bursts displayed a pronounced flickery appearance with external Ba^{2+} and apparent current amplitude was reduced compared to the Ba^{2+}-free patches, as expected for fast block which exceeds the frequency response of the recording system. In addition, traces in the presence of Ba^{2+} displayed numerous, relatively long nonconducting (blocked) intervals which are typi-

cal of a slow block and were not generally observed in similar patches without Ba^{2+}. The voltage dependence of external Ba^{2+} block, illustrated in Fig. 6 *B*, was determined by measuring fractional open time at several potentials between ±60 mV under the conditions of Fig. 6 *A*. This analysis was not affected by the apparent reduction in open channel current amplitude by Ba^{2+} and therefore primarily reflects the slow component of Ba^{2+} block. In the absence of Ba^{2+}, fractional open time was >0.95 at all potentials tested. In the presence of Ba^{2+}, fractional open time decreased as the potential was made more negative at the cell interior, i.e., at potentials which would be expected to drive Ba^{2+} into the channel. At positive cell potentials >20 mV, no effect of Ba^{2+} on fractional open time was evident when compared with similar patches without Ba^{2+}.

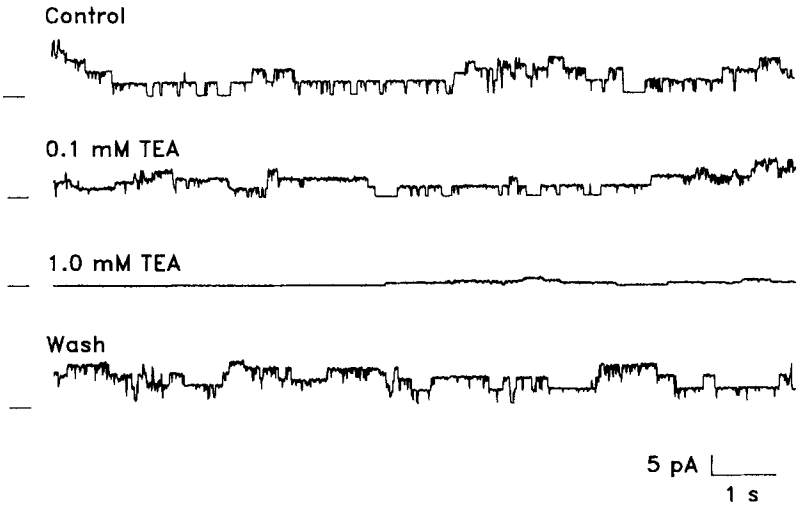

FIGURE 7. Blockade of the large-conductance K^+ channel by extracellular TEA. Traces show outward K^+ currents (upward pen deflection) recorded from an outside-out patch with KCl-EBSS in the pipette and NaCl-EBSS in the bath. Holding potential was 0 mV. Markers at left indicate the current level when all channels were closed. (*Upper trace*) Control currents in the absence of TEA. Addition of 0.1 μM TEA to the bathing solution (*second trace*) slightly reduced the apparent current amplitude and generally increased open channel noise. Currents were nearly abolished by increasing the TEA concentration to 1 mM (*third trace*). The effect of TEA was completely reversed by washing with a TEA-free solution (*lower trace*).

TEA blocked the large-conductance K^+ channel specifically at the extracellular side of the channel. A representative result from five experiments with outside-out patches is shown in Fig. 7. Outward currents were recorded with KCl-EBSS in the pipette and NaCl-EBSS in the bath at a holding potential of 0 mV. TEA (0.1 mM) added to the bathing solution slightly reduced the apparent amplitude of outward K^+ currents and generally increased the noise level of the open state. Increasing the TEA concentration to 1.0 mM reduced current amplitude to extremely low levels, producing virtually complete block. In contrast, similar concentrations of TEA had little or no effect in inside-out patches when added to the solution bathing the

inside membrane (not shown). The effect of TEA in outside-out patches was rapidly and completely reversed by washing TEA out of the bath.

Quinidine produced a flickery, amplitude-reducing block similar to TEA when added to the solution bathing the cytoplasmic membrane in inside-out patches (Fig. 8). In the presence of 100 μM quinidine, the apparent current amplitude was reduced by ~50% and the noise level of the open state was increased. Increasing the quinidine concentration to 1 mM further reduced current amplitude to near zero. The effect of quinidine was rapidly and completely reversed by washing the drug out of the bath. Chlorpromazine (100 μM) or trifluoperazine (100 μM), which block large-conductance, Ca^{2+}-activated K^+ channels in smooth muscle cells (McCann and

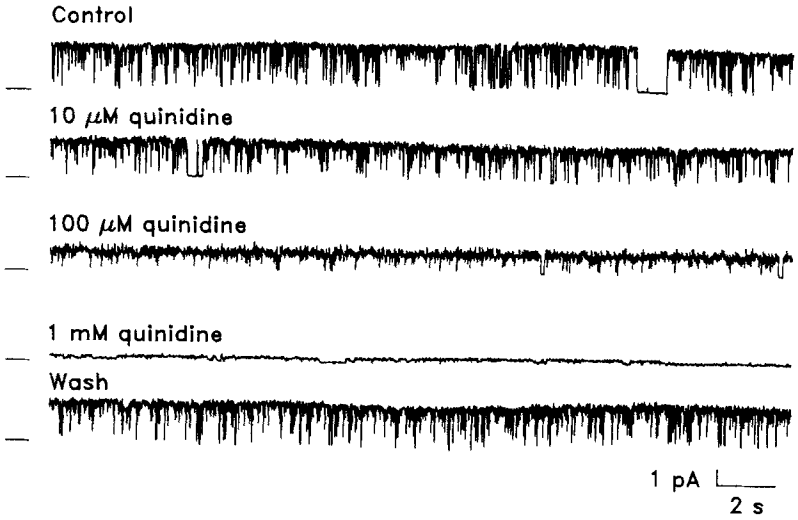

FIGURE 8. Quinidine block of the large-conductance K^+ channel. Traces are from an inside-out patch with KCl-EBSS in the bath and NaCl-EBSS in the pipette at a holding potential of 0 mV. Outward current is indicated by an upward pen deflection. Markers at left indicate the closed channel current level. (*Upper trace*) Outward K^+ current in the absence of quinidine. (*Subsequent traces*) Currents in the presence of 10 μM, 100 μM, and 1 mM quinidine. Quinidine increased the open channel noise level and caused a progressive decrease in apparent current amplitude. As shown in the last trace, the effect of quinidine was rapidly reversed by replacing the bath with quinidine-free solution.

Welsh, 1987), produced a similar but more potent, amplitude-reducing block when added to the inside membrane in inside-out patches, while papaverine (200 μM) produced a slower flickery block which was not accompanied by a reduction in current amplitude (not shown).

K^+ vs. Rb^+ selectivity. We compared the conductance of the channel to K^+ and Rb^+ in excised patches by examining the current-voltage relations in the presence of opposing K^+ and Rb^+ gradients and found that the channel displayed a marked conduction selectivity for K^+ over Rb^+. Fig. 9 shows three current-voltage plots. The first is from an inside-out patch with KCl-EBSS in both the bath and the pipette

(●), where normal inward and outward currents were recorded. The bath was then changed to a similar solution in which KCl was replaced with RbCl (○). Normal inward K^+ currents were still recorded at negative holding potentials (161 pS), but outward Rb^+ currents recorded at positive potentials had a markedly lower conductance (38 pS). Currents reversed near 0 mV. The third plot shows the results obtained from a second inside-out patch in which the K^+/Rb^+ gradients were reversed, i.e., with KCl-EBSS in the bath and RbCl solution in the pipette (△). In this case, normal outward K^+ currents were recorded (141 pS) but inward Rb^+ currents had a slope conductance of only 17 pS. Similar results were obtained in two additional experiments.

Small-Conductance Inwardly Rectifying K^+ Channels

Cell-attached patches. Smaller-conductance K^+ channels were recorded in cell-attached patches but only if the recording conditions were adjusted to allow K^+ to

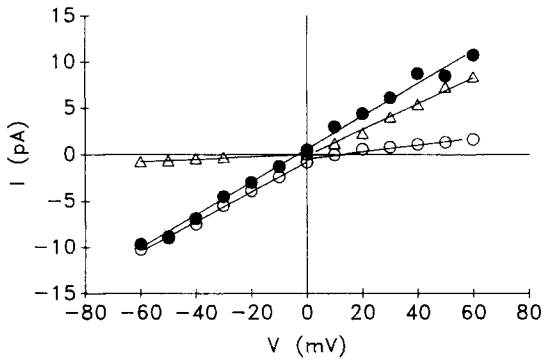

FIGURE 9. Representative current-voltage plots for the large-conductance K^+ channel determined using inside-out patches in the presence of a Rb^+ gradient. (●) *I–V* relation when the patch was bathed with symmetric KCl-EBSS solutions. Slope conductance of inward and outward currents was 174 and 165 pS, respectively. (○) Result of replacing KCl in the bath with RbCl using the same patch. After this maneuver, normal inward K^+ currents were recorded but the conductance of outward currents was reduced from 165 to 38 pS. The reversal potential was near 0 mV. (△) *I–V* relation determined using another patch with RbCl solution in the pipette and KCl-EBSS in the bath. Normal outward K^+ currents were recorded having a slope conductance of 141 pS; however, inward Rb^+ currents had a conductance of only 17 pS.

flow in the inward direction, i.e., from the pipette to the cell interior. Representative currents recorded from a cell-attached patch at a holding potential of 0 mV with KCl-EBSS in the pipette and NaCl-EBSS in the bath are shown in Fig. 10 *A*. Under these recording conditions, the cells were able to develop a normal resting membrane potential. Because the K^+ concentration of the pipette solution was high, i.e., E_K across the membrane patch was approximately zero, the primary driving force for K^+ flow was the resting potential. In the figure, two types of inward K^+ currents can be discerned. One type consists of high-amplitude events that occurred infrequently and were very brief, usually too brief to be fully resolved. These short-duration events could be identified as currents through the large-conductance, Ca^{2+}-activated K^+ channel on the basis of their large single-channel conductance and voltage dependence of gating, i.e., if the patch was depolarized, the open time of these currents increased dramatically. In addition to the large K^+ channel, lower-conductance events with longer open time durations are evident in Fig. 10 *A*. Under

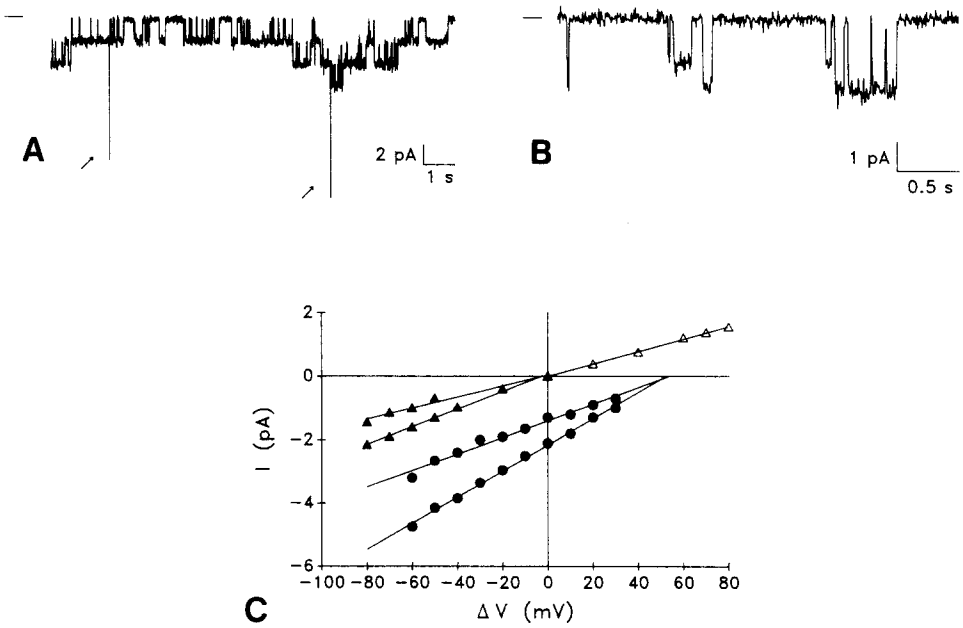

FIGURE 10. (*A*) Inward K^+ currents recorded under "resting" conditions. Trace is from a cell-attached patch with NaCl-EBSS in the bath and KCl-EBSS in the pipette at a holding potential of 0 mV. The primary driving force for inward K^+ flow under these conditions is the resting membrane potential. Channel opening is indicated by a downward pen deflection. Marker at left indicates the closed channel current level. This record was dominated by the opening of three of the smaller-conductance K^+ channels. Infrequent and very brief openings of a large-conductance K^+ channel were also observed in this patch, as indicated by the arrows. (*B*) Smaller-conductance K^+ currents commonly exhibited two distinct current amplitudes. Trace shows inward K^+ currents recorded under conditions identical to 10*A* from a patch which displayed both current levels. (*C*) Representative current-voltage relations for the smaller-conductance K^+ channels. Holding potential was defined as the potential of the cell interior. The slope conductances calculated for the two commonly recorded inward current levels under the conditions in 10B were 41 and 26 pS (●). The apparent reversal potential was ~+50 mV, although actual current reversal was generally not observed, even at holding potentials exceeding +100 mV. From four such plots, the mean slope conductances were 39 ± 2 and 28 ± 3 pS (±SE). On rare occasions, outward current was recorded. The triangles represent currents recorded from a cell-attached patch bathed with symmetric KCl-EBSS solutions in which both inward and outward currents were recorded. Inward currents displayed the characteristic two conductance levels (28 and 18 pS, ▲). Outward currents displayed several conductance levels with the main level having a conductance of ~20 pS (△).

conditions that favored inward K^+ flow, the majority of cell-attached patches contained two or more of these smaller-conductance K^+ channels. These currents often displayed two distinct amplitudes (Fig. 10 *B*). We have not been able to determine unequivocally if the two distinct amplitudes represent two separate channel types or a single channel type having two distinct conductance states. However, both conductances appeared to possess identical characteristics, as if they arose from a single channel type.

The gating of the small-conductance K^+ channels did not exhibit the extreme voltage dependence observed for the large-conductance K^+ channel. Though the fraction of total time spent in the open state appeared to be somewhat lower at hyperpolarized potentials, inward currents were recorded at all negative holding potentials tested (up to -100 mV from resting potential). As a result of bathing the cells in NaCl-EBSS to allow development of a resting potential, the open probability of the large-conductance K^+ channel was negligible due to the strong voltage dependence of gating for that channel. Under the same conditions inward K^+ currents through the relatively voltage-independent, smaller-conductance K^+ channels were easily discernible. As both types of K^+ channels were usually present in most patches, recording at the resting membrane potential allowed us to "isolate" the smaller-conductance K^+ channels from the larger K^+ channels which, if open, would dominate the current records.

The calculated slope conductances of the smaller inward currents under the condition in Fig. 10 *B* were 39 and 28 pS and the apparent reversal potential for both was >50 mV (Fig. 10 *C*). Inward currents with a similar single-channel conductance, apparent reversal potential and frequency of sighting were recorded if the Cl^- in the pipette solution was replaced with the impermeant anion gluconate but were never observed when KCl in the pipette was replaced with NaCl. It is therefore clear that these inward currents were carried by K^+. Currents through the smaller K^+ channels exhibited a very pronounced inward rectification. We were not typically able to resolve outward K^+ currents through this population of channels even in the conditions of a large driving force for outward K^+ flow. For example, in patches where smaller-conductance inward currents were clearly present, we were typically unable to record outward currents, even at holding potentials of $+100$ mV or greater under the conditions in Fig. 10 *C*. This absence of outward currents upon depolarization was clearly observed on numerous occasions in patches which did not contain large K^+ channels (which, if present, would be activated by depolarization and could obscure smaller outward currents). We have therefore referred to the smaller K^+ channel as an inward rectifier. On at least two occasions, however, we recorded outward currents in patches which contained the smaller-conductance K^+ channels (again, in the absence of large K^+ channels). The current voltage relation for one of these is included in Fig. 10 *C* for a cell-attached patch bathed in symmetric KCl-EBSS solutions. These extremely rare sightings may represent outward currents through the inward rectifier. We cannot exclude the possibility that outward currents in this case were carried by a separate population of ion channels that are distinct from the inward rectifier. However, there were similarities between inward and outward currents, including the conductance values and the observation that both displayed subconductance levels, which suggested that the outward currents were carried through the inward rectifiers. If so, the fact that they are seen only on very rare occasions may indicate that the inward rectification characteristic of this channel stems from a tonic inhibitory regulation of channel gating and is not a fundamental conduction characteristic of the channel protein.

Excised patches. In contrast to the stability of the large-conductance K^+ channels in inside-out patches, the smaller conductance K^+ channels typically became inactive immediately after excision of the patch. However, in a few patches, the

channels remained active transiently in the inside-out configuration. In these patches, we attempted to determine if the gating of the small-conductance K^+ channel was regulated by intracellular Ca^{2+}. Replacing NaCl-EBSS bathing the cytoplasmic membrane with a Ca^{2+}-free (+5 mM EGTA) NaCl solution had no apparent effect on open time in these instances.

Blocker specificity. The inability to record currents through the small-conductance K^+ channels in excised patches limited our ability to examine the effects of membrane-impermeant K^+ channel blockers such as Ba^{2+} and TEA. Studies of blocker effects were carried out by recording from cell-attached patches as previously described, i.e., NaCl-EBSS in the bath and KCl-EBSS in the pipette, but with the blockers included in the pipette solution. Since we were unable to change the pipette solution after seal formation, a blocker-free control was not possible using the same patch. We were able, however, to make qualitative comparisons of the blocker specificity of the small-conductance K^+ channels and the large-conductance, Ca^{2+}-activated K^+ channel using this protocol.

TEA included in the pipette at a concentration of 10 mM had no readily discernible effect on currents through the smaller K^+ channels. The normal gating pattern was maintained in the presence of TEA and current amplitudes were comparable to those in blocker-free experiments (not shown). While subtle effects could not be excluded, this agent clearly did not produce the fast, amplitude-reducing block observed for the large-conductance K^+ channel (refer to Fig. 7). Slope conductance of the two commonly recorded conductances determined from five current-voltage plots with 10 mM TEA in the pipette were 36 ± 1 and 22 ± 1 pS, similar to conductances in the absence of TEA. As expected, inward currents through the TEA-sensitive large-conductance K^+ channel were never observed under these conditions.

Barium included in the pipette solution appeared to block currents through the smaller K^+ channels. Fig. 11 shows a typical inward current record in the presence of 5 mM $BaCl_2$. TEA (10 mM) was also included in the pipette solution in these experiments to block currents through the large K^+ channel. Current records in the presence of Ba^{2+} were characterized by rapid flicker, presumably reflecting the blocking and unblocking events. Open durations were obviously reduced compared to the normal gating pattern in the absence of Ba^{2+} (see Fig. 10 *A* for comparison), but block at 5 mM Ba^{2+} was far from complete even though the potential across the patch (i.e., the resting potential) favored Ba^{2+} entry into the channels.

Quinidine permeates cell membranes and can block K^+ channels in cell-attached patches when added to the solution bathing the outside of the cell (Richards and Dawson, 1986). However, quinidine (200 μM) added to the solution bathing isolated salt gland cells had no apparent effect on the gating or amplitude of currents through the small-conductance K^+ channels in three experiments, even though this agent produced its characteristic flickery block of large-conductance K^+ currents present in the same patch. A similar lack of effect was found for 100 μM chlorpromazine or 200 μM papaverine added to the bath.

Effect of Carbachol on Single K^+ Channels

The muscarinic agonist carbachol elicits Cl^- secretion in layers of cultured salt gland cells (Lowy et al., 1985*a*, 1989) and increases intracellular Ca^{+2} levels in freshly iso-

lated salt gland cells (Snider et al., 1986). It was of interest therefore to determine if carbachol would elicit a change in the activity of either of the K^+ channels. One result from five experiments in which carbachol specifically activated the large-conductance K^+ channel is shown in Fig. 12. Inward K^+ currents were recorded in cell-attached patches with KCl-EBSS in the pipette and NaCl-EBSS in the bath. The holding potential was 0 mV, i.e., the potential across the patch was equal to the resting membrane potential. Patches were chosen which clearly contained at least one large-conductance K^+ channel, as evidenced by brief and infrequent inward openings of large amplitude, in addition to the smaller-conductance K^+ channels. Immediately after addition of 100 μM carbachol to the solution bathing the cells, an obvious increase in the open probability of the large-conductance K^+ channel was observed. In this experiment, fractional open time was increased from 0.001 to 0.024 in the presence of carbachol. In two other similar experiments in which this parameter could be calculated, carbachol increased fractional open time from 0.004

FIGURE 11. Blockade of the smaller-conductance K^+ channels by external barium. (*A*) Trace is from a cell-attached patch with NaCl-EBSS in the bath at a holding potential of 0 mV. Marker at left indicates the current level when all channels were closed. The pipette solution was KCl-EBSS with 5 mM $BaCl_2$ and 10 mM TEA. TEA was included to block currents through the large-conductance K^+ channels and was shown previously to have no obvious effects on the gating or amplitude of the smaller-conductance K^+ channels. Single-channel currents in the presence of external Ba^{2+} exhibited a marked flicker compared to the normal gating pattern in Ba^{2+}-free patches. (*B*) The lower trace shows currents in *A* on an expanded time scale, illustrating that the flickery appearance of currents in the presence of external Ba^{2+} arises from a drastic reduction in channel open time.

to 0.236 at a holding potential of 0 mV and from 0.003 to 0.533 at a holding potential of +30 mV. This activation by carbachol was not accompanied by a change in current amplitude (indicating that carbachol did not induce a noticeable shift in steady-state membrane potential) and was readily reversed by changing the bathing solution to one containing 10 μM atropine in the presence of carbachol. The response of the cells to carbachol was variable and many cells did not respond to carbachol stimulation. This variability may reflect, in part, the variable sensitivity of the large-conductance K^+ channels in different patches to cytoplasmic Ca^{2+} (see Fig. 4 *B*).

The effect of carbachol on the smaller K^+ channels was more difficult to assess in these experiments, since the recordings in the presence of carbachol were usually dominated by the larger K^+ channels. The smaller K^+ channels, however, were clearly still opening in the presence of carbachol and we have never observed an obvious effect of carbachol on the gating of these channels. Therefore, although we cannot exclude a more subtle effect of carbachol on the smaller K^+ channels, it is

clear from these experiments that the major effect of this agonist is activation of the large-conductance K^+ channels in salt gland cells.

Blocker Effects on Resting Membrane Potential

To test for the role of K channels in maintaining the resting potential of isolated salt gland cells, the value of the resting potential was estimated by determining the zero current potential for the large-conductance K^+ channels in cell-attached patches

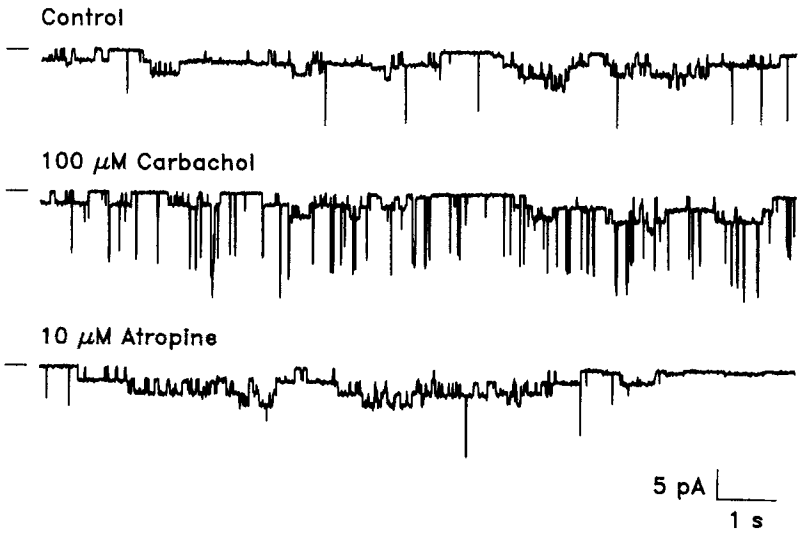

FIGURE 12. Effect of carbachol on single K^+ channels in a cell-attached patch. Traces show inward K^+ currents (downward pen deflection) with KCl-EBSS in the pipette and NaCl-EBSS in the bath at a holding potential of 0 mV. Markers at left indicate the current level when all channels were closed. In the absence of agonist (*upper trace*), at least three smaller-conductance K^+ channels were active. Occasional and very brief openings of a large-conductance K^+ channel were also observed. Immediately after addition of 100 μM carbachol to the solution bathing the cells (*middle trace*), openings of the large K^+ channel increased in frequency. In contrast, carbachol had no obvious effect on currents through the smaller-conductance K^+ channels. The activation of the large K^+ channel was reversed by subsequent addition of 10 μM atropine in the presence of carbachol (*lower trace*).

under conditions where E_K across the patch was near zero. In 22 patches with KCl-EBSS in the pipette and NaCl-EBSS in the bath, both inward and outward K^+ currents were recorded which reversed at 70 ± 3 mV (mean ± SD). Addition of 10 mM TEA to the solution bathing the cells had no effect on the zero current potential (72 ± 2 mV, $n = 5$) but 5 mM $BaCl_2$ reduced it to 50 ± 6 mV ($n = 4$). In all cases, replacing NaCl in the bath with KCl shifted the zero current potential to near zero.

Membrane Location of K^+ Channels

Since it was not possible to morphologically distinguish apical vs. basolateral membrane regions in isolated salt gland cells, we attempted to obtain information

TABLE I

Frequency of Recording K^+ Channels in Cell Layers Vs. in Dissociated Cells

Site of recording	Large K^+	Small K^+
Apical surface of confluent layer	2/25 (0.08)	3/25 (0.12)
Dissociated from confluent layer	14/20 (0.70)	12/20 (0.60)
Freshly dissociated	24/40 (0.60)	29/39 (0.74)

Values are the number of patches in which at least one large- or small-conductance K^+ channel was recorded divided by the total number of patches tested. Recording conditions were as described in Fig. 10.

regarding the membrane location of K^+ channels in these cells by using confluent layers of salt gland cells grown in primary culture. Table I shows the fraction of total patches in which either K^+ channel was recorded in freshly dissociated cells, in patches to the apical membrane surface of confluent layers in primary culture, and in single cells dissociated from confluent layers using EDTA. The table shows that neither K^+ channel was frequently recorded in apical patches but that both were commonly recorded in dissociated cells, including those isolated from confluent layers. These results are compatible with the notion that both the large and the small-conductance K^+ channels normally reside in the basolateral membranes of salt gland cells.

DISCUSSION

Two Types of K^+ Channel in Salt Gland Cells

The presence of multiple K^+ channel types in the basolateral membranes of epithelial cells (Dawson, 1987) complicates the analysis of the role of any particular channel type in cellular transport phenomena. For example, Richards and Dawson (1986, 1987) reported three types of K^+-conducting channels in the membranes of colonic cells, one of which appeared to be active only if the cells were swollen. In the present study, we found that secretory cells from the salt gland contained at least two distinct channel types which were localized in the same patches of membrane but responded differentially to secretagogues, blockers, and membrane potential.

TABLE II

Summary of K^+ Channel Characteristics in Avian Salt Gland Cells

Characteristic	Large K channel	Small K channel
Slope conductance (*pS*)	170	30–40
Rectification	None	Inward
Blockers	Ba	Ba
	TEA	
	Quinidine	
	Chlorpromazine	
	Papaverine	
Ca-activated	Yes	(No)?
Voltage dependence	Strong	Weak
Open at resting potential	No	Yes
Activated by carbachol	Yes	No

One type of K^+ channel had a large conductance, was activated by intracellular Ca^{2+} and was strongly voltage dependent: The other K^+ channel had a smaller conductance, was relatively voltage independent and typically displayed pronounced inward rectification. The properties of both types of K^+ channel are summarized in Table II.

The large-conductance K^+ channel clearly belongs to the general class of Ca^{2+}- and voltage-activated "maxi" K^+ channels which have been found in a wide variety of animal cell types (Latorre and Miller, 1983). In common with many maxi K^+ channels, the large-conductance K^+ channel in the salt gland exhibited a high single-channel conductance (168 pS in symmetric 121 mM K^+ solutions), a pronounced dependency of channel open time on cytoplasmic Ca^{2+}, and a marked voltage dependence of gating such that the open probability increased with membrane depolarization.

Barium blocked this channel from both the intracellular and extracellular faces of the membrane, but was more potent at the inside membrane where it produced a "slow" block; i.e., the duration of blocking events was long relative to the durations of normal openings and closings. The voltage dependence of Ba^{2+} block at either side of the membrane suggests that Ba^{2+} blocked by entering open channels and binding inside so that current flow was obstructed. Evidence for this type of open channel block by Ba^{2+} was obtained for large-conductance K^+ channels in muscle (Vergara and Latorre, 1983; Benham et al., 1985) and cultured kidney cells (Guggino et al., 1987).

In contrast to Ba^{2+}, TEA and quinidine were "fast" blockers of the large-conductance K^+ channel; i.e., the blocking events were frequent and of short duration causing a flickery appearance of the current record and reducing apparent current amplitude as expected if the rate of block and unblock exceeded the frequency response of the recording system. The fast flickery block by quinidine is in contrast to the slower, more potent block by this agent of single K^+ channels in turtle colon epithelial cells (Richards and Dawson, 1986).

The second type of K^+ channel identified in salt gland membranes was a smaller-conductance K^+ channel which typically displayed pronounced inward rectification. This channel was weakly voltage dependent compared with the larger K^+ channel and was open at the normal resting membrane potential. External barium blocked the smaller K^+ channel, but quinidine and TEA had no obvious effect on either gating or current amplitude. Inward-rectifying K^+ channels with similar conduction characteristics have been reported in cardiac cells (Sakmann and Trube, 1984), HeLa cells (Suavé et al., 1983) and lens epithelial cells (Rae, 1988). These channels also display pronounced inward rectification, have similar conductances, and can assume multiple conductance states. Furthermore, they tend to be open at the resting membrane potential (Sakmann and Trube, 1984; Suavé et al., 1983) and, at least in cardiac cells, are distinct from the inward rectifier which is inhibited by ATP (Trube and Hescheler, 1984).

Large K^+ Channel: Possible Role in Agonist-activated Cl^- Transport

Active ion transport by salt gland cells has been studied using confluent layers of cells grown in primary culture and mounted in standard Ussing chambers (Lowy et

al., 1985*a*, 1987, 1989; Lowy and Ernst, 1987). In the absence of an appropriate agonist active ion transport is not detectable, but muscarinic cholinergic agonists, β-adrenergic agonists and VIP evoke an electrical current consistent with active Cl^- secretion from serosa to mucosa. This current is blocked by serosal Ba^{2+} (Lowy et al., 1989) as expected if the inward current due to agonist-evoked Cl^- exit from the cell must be balanced by an outward current carried by K^+ exit from the cell across the basolateral membrane. The observations reported here led us to propose that one of the K^+ channels described in this paper, the large-conductance K^+ channel, functions specifically in agonist-induced secretory responses while the smaller-conductance K^+ channels seem unrelated to the activation of salt transport.

Several observations argue strongly that the large K^+ channel could play a role in the muscarinic secretory response of the salt gland. First, the activation of this channel by carbachol and the antagonism of this effect by atropine parallels the activation and inactivation of net Cl^- transport by the same agents in cultured salt gland cells (Lowy et al., 1985*a*). Both K^+ channel activity and net Cl^- transport remain activated as long as agonist is present but are rapidly inactivated by antagonist. Secondly, an identical cycle is observed for the elevation by carbachol of intracellular free calcium as determined by means of quin-2 flourescence studies (Snider et al., 1986). Carbachol activated a sustained rise in free calcium from 200 to 750 nM which was rapidly restored to baseline by atropine. Thirdly, we have shown here that the large K^+ channel is regulated by cytoplasmic Ca^{2+} at concentrations near those determined from quin-2 experiments in intact cells (Snider et al., 1986) so that it is reasonable to presume that the carbachol-induced increase in K^+ channel open time was due to the increase in intracellular Ca^{2+} elicited by this agent. The open time of the large K^+ channel in cell-attached patches is near zero at the resting potential in untreated cells (e.g., Fig. 12), which is consistent with the calcium and voltage activation characteristics determined in excised patches (Fig. 4 *B*). For example, fractional open time at -60 mV in inside-out patches was close to zero when the Ca^{2+} concentration at the cytoplasmic membrane was held at 100 nM. Increasing Ca^{2+} to 1–10 μM dramatically increased K^+ channel open time. The correlation of carbachol-induced changes in net Cl^- transport, cell calcium and K^+ channel open time argues strongly that the latter event is a normal feature of agonist activated salt transport.

The variable sensitivity of the large-conductance K^+ channels in different patches to cytoplasmic Ca^{2+} was somewhat surprising. A fairly large cell-to-cell variability in regard to activation of large-conductance K^+ channels was reported in lacrimal acinar cells (Marty et al., 1984). In salt gland cells, such variability may underlie the variable response of the K^+ channels to carbachol stimulation. The process of salt adaptation involves dramatic developmental changes which generally occur over a period of 1–2 wk. These changes include increased basolateral membrane infolding (Ernst and Ellis, 1969) and an upregulation of basolateral Na/K ATPase (Ernst and Mills, 1977) and muscarinic receptor binding sites (Hootman and Ernst, 1982). Salt gland suspensions (which generally came from ducks salt-stressed for 1 wk or less) therefore contained cells at various stages of salt stress-induced differentiation (Lowy et al., 1985*b*), and it is conceivable that this developmental variability contributed to the variability observed in both cell-attached and detached patches.

Membrane Location of K^+ Channels

Cell dissociation disrupts cell polarity such that the apical membrane is no longer resolved as a domain that is morphologically distinct from the extensive basolateral membrane. The morphology of the isolated cells in which both types of K^+ channel were commonly recorded was such that the highly infolded basolateral membrane, which is retained after dissociation (Hootman and Ernst, 1980; Lowy et al., 1985*b*), was most likely to be contacted by the pipette. We cannot, of course, exclude "mixing" of apical and basolateral membrane components in the isolated cells. In contrast to the isolated cells, we found that the probability of recording either large- or small-conductance K^+ channels was quite low when patches were formed on the apical membrane surface of confluent salt gland layers in primary culture. These results are consistent with the presumption that both K^+ channel types normally reside in the basolateral membrane. Macroscopic current measurements support this conclusion. In confluent layers of cultured salt gland cells, barium blocks carbachol-induced I_{sc} but only when added to the serosal (basolateral) solution (Lowy et al., 1989).

Large K^+ Channel and the Resting Membrane Potential

Several features of the behavior of the large-conductance K^+ channel are consistent with the notion that this channel does not play a major role in the determination of the membrane potential under "resting" conditions, i.e., in the absence of agonist. The voltage and calcium dependence of the channel gating suggests that the fractional open time would be very near zero if the membrane potential were <-60 mV, inside negative at an intracellular Ca^{2+} concentration in the vicinity of 100 nM. Although the membrane potential of the cells in the intact gland is unknown, that of the isolated cells can be estimated to be ~-70 mV from the reversal potential for currents through the large-conductance K^+ channel when $E_k = 0$ (high K^+ in the pipette). This resting potential was shifted to zero by raising external K^+ concentration but it was unaffected by TEA at a concentration (10 mM) which would be expected to produce complete block of the large-conductance K^+ channels. These observations are consistent with the notion that the Ca^{2+}-activated K^+ channels in salt gland cells provide a pathway for outward K^+ current which is only present under stimulated conditions.

K^+ Channels in Cl^- Secretory Epithelia

K^+ channels have been identified in the basolateral membranes of several Cl^- secretory epithelia but their properties and regulation are by no means uniform. Large-conductance, Ca^{2+}- and voltage-regulated K^+ channels similar to the one reported here in salt gland cells have been described in exocrine pancreas (Maruyama et al., 1983*b*), salivary gland (Maruyama et al., 1983*a*), and lacrimal gland (Findlay, 1984, Marty et al., 1984). The large K^+ channels in these cell types have a blocker profile (e.g., Iwatsuki and Petersen, 1985*a*, *b*, Trautmann and Marty, 1984) and K^+ vs. Rb^+ selectivity (Findlay, 1984, Gallacher et al., 1984) identical to that reported here for salt gland cells. Furthermore, muscarinic receptor activation in these cells appears to be coupled to K^+ channel activation via increased intracel-

lular Ca^{2+} (Maruyama et al., 1983*b*; Findlay, 1984; Marty et al., 1984; Trautmann and Marty, 1984; Gallacher and Morris, 1986). However, different types of K^+ channels have been described in the basolateral membranes of other Cl^- secretory epithelia. K^+ channels in tracheal epithelial cells have a relatively small conductance and are not voltage regulated (Welsh and McCann, 1985). These channels are regulated by cytoplasmic Ca^{2+}, though the role of Ca^{2+} in Cl^- secretion by tracheal epithelia is unclear. In rectal gland, basolateral K^+ channels have been reported which have a large conductance but are apparently not regulated by either Ca^{2+} or voltage (Gögelein et al., 1987; Greger et al., 1987).

Possible Role for the Inward Rectifier

The issue of the K^+ channels responsible for maintaining the K^+-dependent resting membrane potential in salt gland cells has not been resolved. The Ca^{2+}- and voltage-activation characteristics of the large-conductance K^+ channels suggest that they are activated only when the cells are in a secretory state. On the other hand, the smaller-conductance K^+ channels, which are apparently unaffected by carbachol, are open at normal resting membrane potentials and may therefore be involved in the development of the resting potential. However, these channels typically displayed pronounced inward rectification. It is possible that the conditions of this study prevented us from detecting outward current flow through these channels. For example, Payet et al. (1985) found that outward currents through the inward rectifier in cardiac cells could not be recorded if the K^+ concentration in the pipette solution was >75 mM. On rare occasions, we have recorded what appears to be outward current through the inward rectifier channels in salt gland cells, supporting the possibility of a contribution by these channels to the resting potential.

The authors gratefully acknowledge Donna M. Van Lare, James H. Schreiber, and Michael D. Urich for technical assistance.

This study was supported by National Institute of Diabetes and Digestive and Kidney Diseases grants DK-29786 to D. C. Dawson and DK-27559 to S. A. Ernst, and by the University of Michigan Gastrointestinal Peptide Research Center. N. W. Richards was the recipient of National Research Service Award DK-07664. R. J. Lowy was the recipient of National Research Service Award DK-07847.

Original version received 5 May 1988 and accepted version received 3 January 1989.

REFERENCES

Benham, C. D., T. B. Bolton, R. J. Lang, and T. Takewaki. 1985. The mechanism of action of Ba^{2+} and TEA on single Ca^{2+}-activated K^+-channels in arterial and intestinal smooth muscle membranes. *Pflügers Archiv.* 403:120–127.

Bezanilla, F. 1985. A high capacity data recording device based on a digital audio processor and a videocassette recorder. *Biophysical Journal.* 47:437–441.

Chang, D., P. S. Hsieh, and D. C. Dawson. 1988. CALCIUM: a program in BASIC for calculating the composition of solutions with specified free concentrations of calcium, magnesium and other divalent cations. *Computers in Biology and Medicine.* 18:351–366.

Dawson, D. C. 1987. Properties of epithelial potassium channels. *In* Current Topics in Membranes and Transport. Vol. 28. G. Giebisch, editor. Academic Press Inc., New York. 41–71.

Ernst, S. A., and R. A. Ellis. 1969. The development of surface specialization in the secretory epithelium of the avian salt gland in response to osmotic stress. *Journal of Cell Biology.* 40:305–321.

Ernst, S. A., and J. W. Mills. 1977. Basolateral plasma membrane localization of ouabain-sensitive sodium transport sites in the secretory epithelium of the avian salt gland. *Journal of Cell Biology.* 75:74–94.

Findlay, I. 1984. A patch-clamp study of potassium channels and whole-cell currents in acinar cells of the mouse lacrimal gland. *Journal of Physiology.* 350:179–195.

Gallacher, D. V., Y. Maruyama, and O. H. Petersen. 1984. Patch-clamp study of rubidium and potassium conductances in single cation channels from mammalian exocrine acini. *Pflügers Archiv.* 401:361–367.

Gallacher, D. V., and A. P. Morris. 1986. A patch-clamp study of potassium currents in resting and acetylcholine-stimulated mouse submandibular acinar cells. *Journal of Physiology.* 373:379–395.

Gögelein, H., R. Greger, and E. Schlatter. 1987. Potassium channels in the basolateral membrane of the rectal gland of *Squalus acanthias:* regulation and inhibitors. *Pflügers Archiv.* 409:107–113.

Greger, R., H. Gögelein, and E. Schlatter. 1987. Potassium channels in the basolateral membrane of the rectal gland of the dogfish (*Squalus acanthias*). *Pflügers Archiv.* 409:100–106.

Guggino, S. E., W. B. Guggino, N. Green, and B. Sacktor. 1987. Blocking agents of Ca^{2+}-activated K^+ channels in cultured medullary thick ascending limb cells. *American Journal of Physiology.* 252:C128–C137.

Hamill, O. P., A. Marty, E. Neher, B. Sakmann, and F. J. Sigworth. 1981. Improved patch-clamp techniques for high-resolution current recording from cells and cell-free membrane patches. *Pflügers Archiv.* 391:85–100.

Hokin, M. R., and L. E. Hokin. 1967. The formation and continuous turnover of a fraction of phosphatidic acid on stimulation of NaCl secretion by acetylcholine in the salt gland. *Journal of General Physiology.* 50:793–811.

Hootman, S. R., and S. A. Ernst. 1980. Dissociation of avian salt gland: separation procedures and characterization of dissociated cells. *American Journal of Physiology.* 238:C184–C195.

Hootman, S. R., and S. A. Ernst. 1981. Effect of methacholine on Na^+ pump activity and ion content of dispersed avian salt gland cells. *American Journal of Physiology.* 241:R77–R86.

Hootman, S. R., and S. A. Ernst. 1982. [^{3}H]QNB binding to muscarinic receptors in intact avian salt gland cells. *American Journal of Physiology.* 243:C254–C261.

Iwatsuki, N., and O. H. Petersen. 1985*a*. Action of tetraethylammonium on calcium-activated potassium channels in pig pancreatic acinar cells studied by patch-clamp single-channel and whole cell current recording. *Journal of Membrane Biology.* 86:139–144.

Iwatsuki, N., and O. H. Petersen. 1985*b*. Inhibition of Ca^{2+}-activated K^+ channels in pig pancreatic acinar cells by Ba^{+2}, Ca^{2+}, quinine and quinidine. *Biochimica et Biophysica Acta.* 819:249–257.

Latorre, R., and C. Miller. 1983. Conduction and selectivity in potassium channels. *Journal of Membrane Biology.* 71:11–30.

Lowy, R. J., D. C. Dawson, and S. A. Ernst. 1985*a*. Primary culture of duck salt gland. II. Neurohormonal stimulation of active transport. *American Journal of Physiology.* 249:C41–C47.

Lowy, R. J., D. C. Dawson, and S. A. Ernst. 1989. Mechanism of ion transport by avian salt gland primary cell cultures. *American Journal of Physiology.* In press.

Lowy, R. J., and S. A. Ernst. 1987. β-Adrenergic stimulation of ion transport in primary cultures of avian salt glands. *American Journal of Physiology.* 252:C670–C676.

Lowy, R. J., J. H. Schreiber, D. C. Dawson, and S. A. Ernst. 1985*b*. Primary culture of duck salt gland. I. Morphology of confluent cell layers. *American Journal of Physiology.* 249:C32–C40.

Lowy, R. J., J. H. Schreiber, and S. A. Ernst. 1987. Vasoactive intestinal peptide stimulates ion transport in avian salt gland. *American Journal of Physiology.* 253:R801–808.

Marty, A., Y. P. Tan, and A. Trautmann. 1984. Three types of calcium-dependent channel in rat lacrimal glands. *Journal of Physiology.* 357:293–325.

Maruyama, Y., D. V. Gallacher, and O. H. Petersen. 1983*a*. Voltage and Ca^{2+}-activated K^+ channel in baso-lateral acinar cell membranes of mammalian salivary glands. *Nature.* 302:827–829.

Maruyama, Y., O. H. Petersen, P. Flanagan, and G. T. Pearson. 1983*b*. Quantification of Ca^{2+}-activated K^+ channels under hormonal control in pig pancreas acinar cells. *Nature.* 305:228–232.

McCann, J. D., and M. J. Welsh. 1987. Neuroleptics antagonize a calcium-activated potassium channel in airway smooth muscle. *Journal of General Physiology.* 89:339–352.

Payet, M. D., E. Rousseau, and R. Suavé. 1985. Single-channel analysis of a potassium inward rectifier in myocytes of newborn rat heart. *Journal of Membrane Biology.* 86:79–88.

Peaker, M., and J. L. Linzell. 1975. *In* Salt Glands in Birds and Reptiles. Cambridge University Press, Cambridge. 34–66.

Rae, J. L. 1988. An inwardly rectifying potassium channel in chick lens epithelium. *Biophysical Journal.* 53:547*a*. (Abstr.)

Richards, N. W., and D. C. Dawson. 1986. Single potassium channels blocked by lidocaine and quinidine in isolated turtle colon epithelial cells. *American Journal of Physiology.* 251:C85–C89.

Richards, N. W., and D. C. Dawson. 1987. Two types of Ca-activated channel in isolated turtle colon epithelial cells. *Biophysical Journal.* 51:344*a*. (Abstr.)

Sakmann, B., and G. Trube. 1984. Conductance properties of single inwardly rectifying potassium channels in ventricular cells from guinea-pig heart. *Journal of Physiology.* 347:641–657.

Snider, R. M., R. M. Roland, R. J. Lowy, B. W. Agranoff, and S. A. Ernst. 1986. Muscarinic receptor-stimulated Ca^{2+} signaling and inositol lipid metabolism in avian salt gland cells. *Biochimica et Biophysica Acta.* 889:216–224.

Suavé, R., G. Roy, and D. Payet. 1983. Single channel K^+ currents from HeLa cells. *Journal of Membrane Biology.* 74:41–49.

Trautmann, A., and A. Marty. 1984. Activation of Ca-dependent K channels by carbamoylcholine in rat lacrimal glands. *Proceedings of the National Academy of Sciences.* 81:611–615.

Trube, G., and J. Hescheler. 1984. Inward-rectifying channels in isolated patches of the heart cell membrane: ATP-dependence and comparison with cell-attached patches. *Pflügers Archiv.* 401:178–184.

Vergara, C., and R. Latorre. 1983. Kinetics of Ca^{2+}-activated K^+ channels from rabbit muscle incorporated into planar bilayers: evidence for a Ca^{2+} and Ba^{2+} blockade. *Journal of General Physiology.* 82:543–568.

Welsh, M. J., and J. D. McCann. 1985. Intracellular calcium regulates basolateral potassium channels in a chloride-secreting epithelium. *Proceedings of the National Academy of Sciences.* 82:8823–8826.